

## Laser Sintering Model for Composite Materials

J. C. Nelson, N. K. Vail and J. W. Barlow  
Department of Chemical Engineering  
The University of Texas at Austin

### Abstract

A computer model for the sintering of ceramic/polymer composite materials has been established based on empirical sintering rate data. The model calculates sintering depths which result from variations in the operating parameters which include laser power, beam speed, scan spacing, scan vector length, and initial temperatures of the powder and surroundings. Sintering depths measured in multiple layer parts made of polymer coated ceramic powders are compared to sintering depths calculated by the sintering model.

### Introduction

In this paper, the development of a sintering model for composite materials is examined. The sintering model for composites is based strongly on a previously developed model which calculates the extent of sintering and subsequent densification of amorphous polymer powders in response to Selective Laser Sintering (SLS) operating conditions and scanning parameters [Nelson, 1993].

Composite materials are comprised of a non-sintering phase, ceramic or metal, and a sintering phase, polymer. The non-sintering phase is either mixed or coated with the polymer prior to sintering. As the laser scans the composite powder during the part build, the polymer is selectively melted, and upon cooling, solidifies binding the non-sintering phase together. Post-processing of green<sup>1</sup> SLS part removes the polymer phase and bonds the ceramic or metal in a homogeneous phase.

The material system examined in this paper is a ceramic/polymer composite. The ceramic is Silicon Carbide (SiC), and the polymer is poly(methyl methacrylate). The polymer is polymerized in emulsion form, and in a subsequent step, the SiC powder is coated with a thin layer of polymer in a spray dryer. Twenty-five volume percent polymer is applied to the ceramic powder in the spray drying step, then uncoated ceramic is added to reduce the polymer content to twenty volume percent.

### Sintering Model

The development of a computer model is crucial in the understanding and future automation of the SLS process. The sintering model is used as a tool to investigate how the various process variables (i.e. scan speed, laser power, and scan spacing) effect the quality of the finished SLS parts. A sintering model also allows one to perform a

---

<sup>1</sup>A "green" part refers to the state of the SLS object after removal from the sintering machine but before undergoing any post-processing steps.

parametric analysis to study how variations in one parameter affect the sintering depths within a powder layer.

The first building block, used to model the thermal gradients in the SLS powder bed, is the differential equation for thermal diffusion. The differential equation is written in one-dimension as follows:

$$\rho_{(\varepsilon)} C_{P(T)} \frac{\partial T_{(z,t)}}{\partial t} - \frac{\partial}{\partial z} \left( K_{(T,\varepsilon)} \frac{\partial T_{(z,t)}}{\partial z} \right) = G_{(z,t)} \quad (1)$$

$$-K \frac{\partial T}{\partial z} = Q_{(0,t)} + h(T - T_{\infty}) \quad \text{at } z = 0, \quad t > 0 \quad (2)$$

$$-K \frac{\partial T}{\partial z} = 0 \quad \text{at } z = L, \quad t > 0 \quad (3)$$

where  $\rho$  is the bed density at position  $z$ ,  $C_p$  is the specific heat,  $K$  is the thermal conductivity,  $T$  the temperature,  $t$  the time,  $G$  is the internal heat source,  $Q$  the heat source term at the surface, and  $h$  the heat transfer coefficient which includes contributions from both convection and radiation transfer at the surface, and  $T_{\infty}$  the ambient temperature. The flux term,  $Q$ , represents the energy input from the laser as a function of the laser power, laser spot size, scan speed, and scan spacing.

The thermal-diffusion equation, Equation (1), is used to calculate the thermal profiles within a solid region as a function of the thermal properties of the material and the boundary conditions. However, during sintering the material properties change as a function of the void fraction, or porosity, within the solid. Therefore, the material properties are calculated as a function of both temperature and void fraction. The porosity is related to the bed density,  $\rho$ , and the material solid density,  $\rho_s$ , by the expression,

$$\varepsilon = \frac{(\rho_s - \rho)}{\rho_s} \quad (4)$$

and is a function of the powder size distribution, the powder aspect ratio, and the fraction of sintering that has occurred.

The second building block is the sintering model which is used to calculate the change in void fraction as a function of temperature. Several theoretical models are available to model sintering; however, these models are not adequate for powders with broad particle size distributions, or more importantly for composite materials. The sintering rate used in this study is an empirical rate measured using an oven sintering apparatus, [Nelson, 1990; Nelson 1993]. Sintering rate data is acquired at several temperatures 10 to 50 K above the  $T_g$  or  $T_m$  of the material. The temperature dependence of the sintering rate is calculated, and the rate data is extrapolated into the regime where sintering occurs during laser processing.

This method works very nicely for homogeneous polymeric materials (i.e. polycarbonate), however, because the composite material is primarily a ceramic phase, which sinters at very high temperatures relative to the polymer phase, the total densification during oven sintering at the highest operating temperatures was only about 5 percent. Since the amount of sintering was so small, the uncertainty in the extrapolated

rate data was large. For this reason, we measured the sintering rate of a sample of polymer binder in powder form.

Therefore, instead of measuring the rate at which the composite material sinters, we obtained the sintering rate of the binder. Our next task, was to relate the polymer sintering rate to the composite sintering rate. After proposing several models for the interactions that may occur during the sintering of ceramic agglomerates coated with a polymer binder, we settled on a very simple model. Basically, the ceramic and the polymer are treated as two separate powders, and the change in void fraction only occurs in the polymer phase. By this approximation, if the polymer phase completely sinters to full density, the overall change in void fraction is proportional to the amount of polymer present. In our study, the complete sintering of polymer results in the complete sintering of 20 percent of the composite material.

The two building blocks described above, the thermal diffusion equation and the sintering rate equation, are combined in a one-dimensional finite element program optimized to model powder sintering. This transient model calculates the temperature profiles within the powder bed during SLS processing. Within each time step, the temperature profile is used to compute the degree of sintering at each node, and any changes in porosity are calculated. The simulation is complete when the temperature of the powder bed drops below the softening temperature of the polymer where sintering no longer occurs.

### Material Properties

In order to model sintering and the subsequent densification during SLS processing, four pieces of information about the material system must be known which are the thermal conductivity, specific heat, density, and sintering rate of the composite material. Traditionally, the thermal properties of powders are not readily available, therefore, methods of measurement and calculation of the thermal properties must be examined. Calculation of the thermal properties of a powder poses several challenges. The fact that the material system focused upon in this paper is a composite, increases the difficulty of calculation. Techniques for measurement and prediction of the thermal properties needed for the development of a sintering model are presented below.

#### *Density*

The solid density of the composite material is calculated as a function of densities of the individual materials,

$$\rho_s = \phi \rho_{pmma} + (1 - \phi) \rho_{SiC} \quad (5)$$

where  $\phi$  is the volume fraction of polymer binder. For our material system, the polymer comprises 20 percent of the total volume and has a density of 1.2 g/cm<sup>3</sup>. The ceramic, Silicon Carbide has a solid density of 3.217 g/cm<sup>3</sup>. Therefore the solid density of the composite material is 2.81 g/cm<sup>3</sup> by Equation (5).

The density of the agglomerated powder is calculated as a function of the solid density and the powder porosity, Equation (4). The initial porosity of the powder bed is 0.5, which corresponds to a density of 1.41 g/cm<sup>3</sup>. As the porosity decreases, the density of the powder bed approaches the solid density of the composite.

### Specific Heat

The specific heat of the composite is calculated as the mass average of the specific heats of each phase,

$$C_P = \xi C_{P(pm)} + (1 - \xi) C_{P(sic)} \quad (6)$$

where  $\xi$  is the weight fraction of polymer binder. For the composite material system, the weight fraction of polymer is 0.085, which corresponds to a volume fraction of 0.20 polymer. The weight fraction and the volume fraction are related by the following,

$$\phi_1 = \frac{\rho_2 \xi_1}{\rho_2 \xi_1 + \rho_1 (1 - \xi_1)} \quad (7)$$

where the two components are designated by the subscripts 1 and 2.

The specific heat of a material can be readily measured using a DSC (Differential Scanning Calorimeter) or similar apparatus. Figure 1 presents specific heat data for each phase (solid lines) and for the composite (dashed line). The specific heat of PMMA was unavailable at the time of the simulation, therefore, the specific heat of polycarbonate was used in the calculations. The specific heat of the polymer is double that of the silicon carbide. The specific heat of the composite calculated from a mass average of the two components agrees fairly well with the measured data.

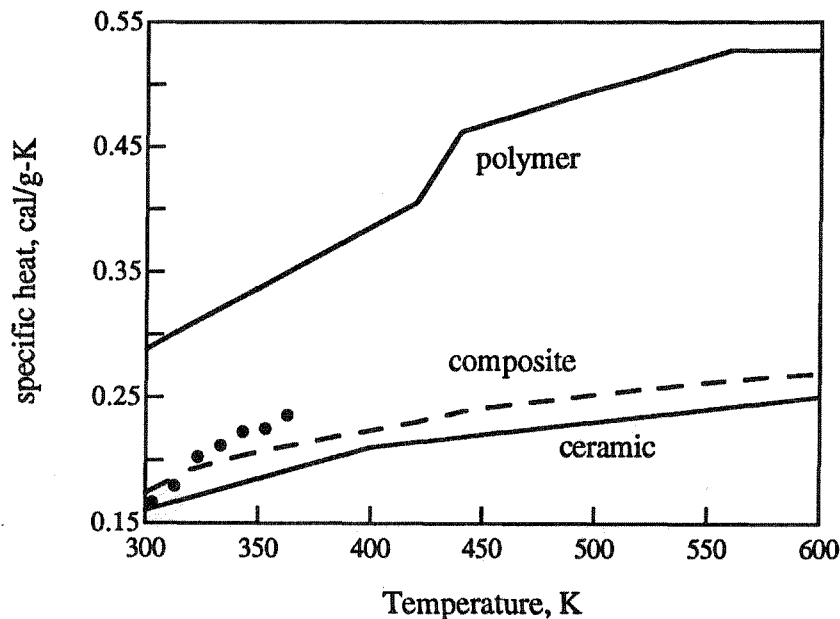


Figure 1 Effective specific heat of the powder bed. The markers (●) represent data measured using a DSC. The specific heat of the composite calculated by a mass average is represented by a dashed line.

### Thermal Conductivity

For most solid materials, thermal conductivity data is reported at one or more temperatures. However, the thermal conductivity data for powders is not readily available. Therefore, the properties of powder must be measured or modeled. The transient heat conduction method [Naumann, 1983] is one method used to measure thermal conductivity of a powder. The transient method is used by Xue, [Xue, 1991], to measure thermal conductivity of powders used in the SLS process. The data reported below for the SiC/PMMA system was measured by Xue using a water bath method and a laser-heated method, [Shi, 1993]. In Figure (1), thermal conductivity data measured by both methods is reported for the composite material at a bed void fraction,  $\epsilon$ , of 0.53. The water bath method and the laser heating method are represented by circles (●) and diamonds (◆), respectively. The water bath method is limited to temperatures below 100 °C; however, the laser heat method allows the measurement of thermal properties at higher temperatures. The sharp increase in thermal conductivity above 100 °C is due to the sintering of the polymer, and the improved contact between Silicon Carbide (SiC) particles.

The model considered for the calculation of the thermal conductivity was published in 1957 by Sakae Yagi and Daizo Kunii [Yagi, 1957] at The University of Tokyo. Yagi and Kunii presented a theoretical model for the effective thermal conductivity of packed beds. The influence of both packing characteristics and temperature on the effective thermal conductivity was studied by comparisons with experimental data. The general equation derived is reduced to the following in the case of gas-filled voids in a motionless fluid:

$$\frac{k_e^o}{k_g} = \frac{\beta(1-\epsilon)}{\gamma\left(\frac{k_g}{k_s}\right) + \frac{1}{\frac{1}{\phi} + \frac{D_p h_{rs}}{k_g}}} + \epsilon\beta \frac{D_p h_{rv}}{k_g} \quad (8)$$

where  $k_e^o$  is the effective thermal conductivity of the powder,  $k_g$  and  $k_s$  are the thermal conductivity of the gas and the solid respectively,  $\epsilon$  is the void fraction of the powder bed,  $D_p$  is the average particle diameter,  $h_{rv}$  and  $h_{rs}$  are the radiation heat transfer coefficients for void to void and solid surface to solid surface, and the remaining variables describe the geometry of the packing. The factor  $\gamma$  is defined as the effective length of solid relating to thermal conduction, divided by the mean diameter of the solid. The factor  $\beta$  is defined as the ratio of the average length between the centers of two neighboring solids in the direction of heat flow, to the mean diameter of the packing. The factor  $\phi$  is defined as the ratio of the effective thickness of fluid film through which heat is conducted to the mean diameter of the packing material. The geometric factors were found by analyzing experimental data reported for effective thermal conductivity, and correlating the data with the theoretical equations. Values of  $\phi$  are calculated as a function of void fraction,  $\epsilon$ , from experimental data previously reported for air. The data conforms to Equation (9).

$$\phi = 0.1927 \times \epsilon^{1.8544} \quad (9)$$

The values of both  $\beta$  and  $\gamma$  are approximately unity, for all cases where the packing particles were either spherical or cylindrical.

Table 1 summarizes the solid and gas thermal conductivity data used to calculate the thermal conductivity of the powder. Because the Yagi-Kunii model, Equation (8), considers only one material, the thermal conductivity of the ceramic and the polymer must be consolidated into an effective thermal conductivity,  $k_{s,eff}$ , of the solid composite material. The effective thermal conductivity of the composite is then used to calculate the effective thermal conductivity of the powder. Two methods are used to calculate the effective thermal conductivity of the solid. First, a simple volume average of the solid thermal conductivity data is considered, Equation (10). As shown in the fifth column of Table 1, this method heavily weights the thermal conductivity of the ceramic. The second method consists of a more complex means of calculating an equivalent thermal conductivity. Based on the assumption that each ceramic particle is evenly coated with polymer, a one-dimensional resistance model is defined, and the effective thermal conductivity is calculated by integrating the thermal conductivity through the particle, [Badrinarayan, 1990]. This method heavily weights the thermal conductivity of the polymer, because all of the heat conducted through the particle must pass through a thin film of polymer. As the thickness of the polymer coating increases, the effective thermal conductivity of the particle approaches that of the polymer.

$$k_{s,eff} = (\phi)k_{s,pmma} + (1 - \phi)k_{s,SiC} \quad (10)$$

**Table 1** Thermal conductivity data used in calculate the effective thermal conductivity in Figure 2. The composite material is 20 percent by volume polymer. thermal conductivity,  $k$  (W/m-K)

Temperature, K	solid material, $k_s$		gas, $k_g$	composite material (SiC/PMMA), $k_{s,eff}$	
	SiC	PMMA	Air	volume average	equivalent conductivity <sup>‡</sup>
300 (27 °C)	456.3	0.195	0.026	368.3	3.04
370 (97 °C)	383.4	0.248	0.031	309.5	3.64
440 (167 °C)	310.6	0.30 <sup>†</sup>	0.036	250.7	4.23

<sup>†</sup> extrapolated

<sup>‡</sup> method derived by Badrinarayan, 1990

Figure 2 compares the measured and calculated effective thermal conductivity of a randomly packed bed of coated ceramic particles. The lines represent the thermal conductivity calculated using the Yagi-Kunii model in conjunction with the effective thermal conductivity of the solid listed in Table 1. The void fraction of the powder bed is decreased linearly from 0.53 (370 K) to 0.41 (420 K) to account for sintering of the polymer phase. The change in void fraction is based on density measurements made by Xue. Although there is a significant difference between the effective thermal conductivity of the composite, the effective thermal conductivity of the powder differs by approximately 20 percent. However, the thermal conductivity model fails to capture the true temperature dependence of the composite material.

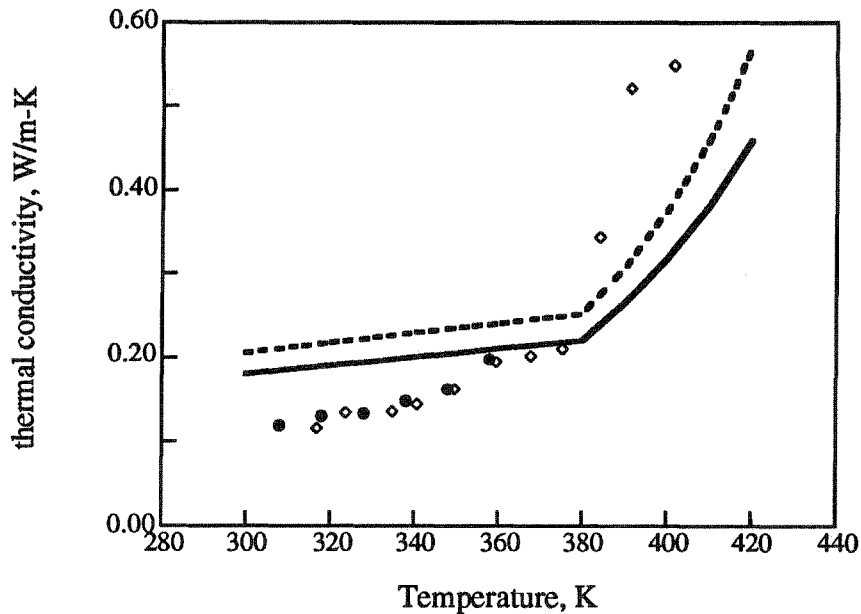


**Figure 2** Effective thermal conductivity of the powder bed where the SiC particles are coated with 20 % by volume PMMA, and the void fraction is 0.53. The markers represent data measured by the (●) water bath method, and the (◇) laser heating method. The lines represent values of thermal conductivity calculated using the Yagi-Kunii model. The solid thermal conductivity used in the model is either (---) a volume average, or (—) an equivalent conductivity, see Table 1.

### *Sintering Rate*

The sintering rate measurement is a key element in the sintering model. Figure 3 shows rate data for both pure PMMA powder and for the composite spray dried powder. The data points represent isothermal rate measurements made using an oven sintering apparatus. The temperatures at which the experiment was performed ranged from 100 to 150 °C. The temperature range used is dependent on the softening temperature of the binder (low value) and the viscosity of the binder (high). Below the softening temperature no sintering occurs. And at higher temperatures, sintering occurs too quickly, and may finish before the sample reaches an equilibrium temperature. Typically, the operating range is between 10 to 50 °C above the softening temperature of the binder.

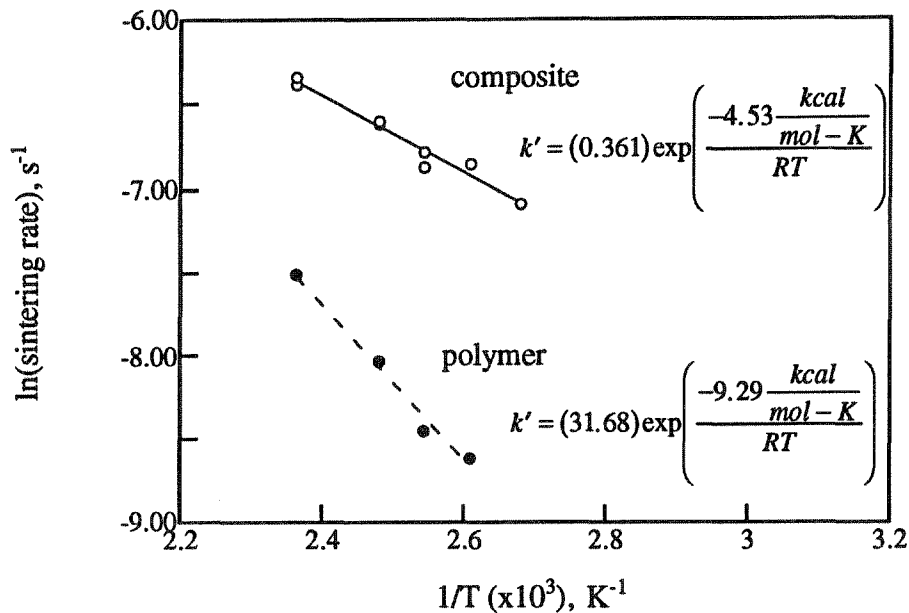


Figure 3 Sintering rate data for both polymer (PMMA) powder and composite (SiC/PMMA) spray dried powder.

### Results and Discussion

Analyzing the results posed several challenges. First, during the actual SLS processing of the composite material, there is no noticeable change in density. Consequently, the density of the green part is the same as that of the unsintered powder. This negligible change in density during SLS processing prevents the direct comparison of sintering model results to the experimental data. For example, in the case of the amorphous sintering model [Nelson, 1993], a direct comparison was made between the density of a SLS part to the density calculated by the sintering model. However, this correlation cannot be made for the composite materials.

Therefore, another means of comparing model results to a measurable parameter has to be established. Bending strength data is available for SiC/PMMA composite SLS parts as well as pictures of the fracture surfaces, [Vail, 1993]. In order to compare the sintering model results to this experimental data, the SLS operating parameters used to make the composite parts via SLS, are used to calculate the surface boundary condition in the model. For the sintering model, a void fraction profile is obtained after the sintering is complete.

To reduce the number of variables in the analysis, the SLS operating parameters are reduced to an energy per unit area,  $\mathcal{A}_N$  (cal/cm<sup>2</sup>), Equation (11). Figure 4 compares both the bending strength of SLS green parts and the percent change in void fraction of the fusible material to the energy flux.

$$\mathcal{A}_N = \frac{\text{laser power}}{(\text{beam speed})(\text{scan spacing})} \quad (11)$$

Both curves increase as the energy flux increases, which is the expected response. In Figure 4a, the change in the initial void fraction of the polymer phase is plotted versus the energy input. As the energy flux is increased, the powder reaches higher temperatures leading to more sintering. In Figure 4b, as the energy flux increases, the strength of the SLS parts increases leveling off at higher values of  $\mathcal{A}_N$ .

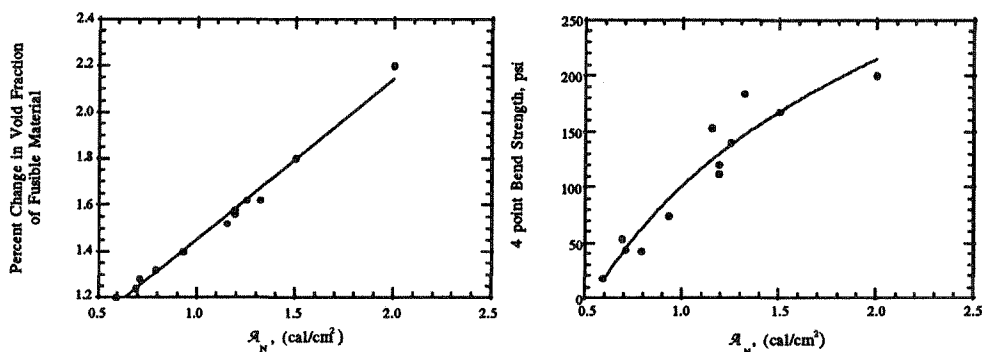


**Figure 4** Effects of an increase in the energy per unit area delivered by the laser during a part build. The predicted change in void fraction (left), and the measured bending strength of test bars via SLS processing (right).

The data in Figure 4 can be replotted by relating the two curves by their common variable,  $\mathcal{A}_N$ . Based on the assumption that the strength increases as the void fraction decreases, the sintering model accurately predicts the expected trends.

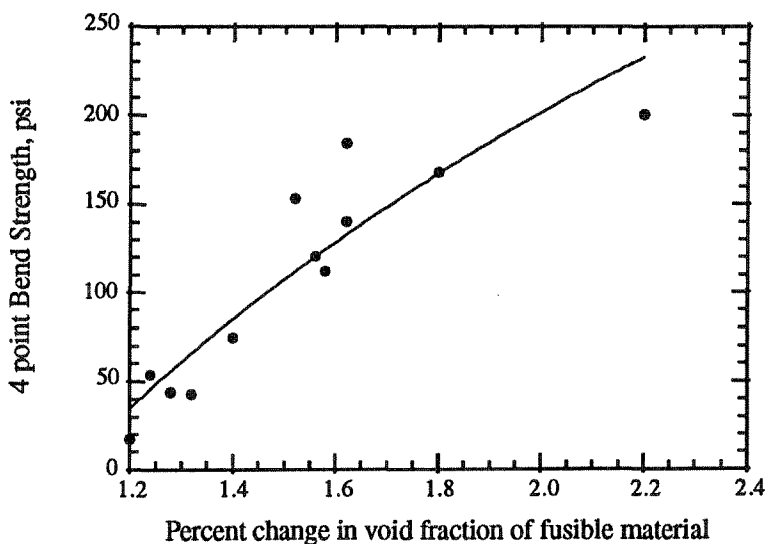


**Figure 5** Comparison of model results to measured bending strengths.

## Summary

The task of developing a laser sintering model for composite materials has presented several challenges. A very simple sintering model to explain void reduction is used because of a lack of information about the sintering of polymer coated agglomerates. The thermal properties of the composite material are calculated from the material properties of each phase. The material properties and the sintering rate data for the composite material are combined in a sintering model which calculates temperature and void fraction profiles in one-dimension. The results of the numerical analysis compare favorably to the measured bending strengths of composite test bars via SLS. The general trends of increasing strength and decreasing void fraction are compared over a range of SLS operating parameters. Future modeling should focus on the interactions between particles and agglomerates during two phase sintering.

## References

- Badrinarayan, B. and Barlow, J. W., "Prediction of the Thermal Conductivity of Beds which Contain Polymer Coated Metal Particles", In *Solid Freeform Fabrication Symposium Proceedings*, pp. 91-98, 1990.
- Naumann, D. and Seydel, K., "Messung der Wärmeleitfähigkeit von Pulvern (Measurement of Thermal Conductivity of Powders)," *Plaste and Kautschuk*, **30**, pp. 233-234, 1983.
- Nelson, J. C. and Barlow, J. W., "Sintering Rates in the Selective Laser Sintering Process" In *Solid Freeform Fabrication Symposium Proceedings*, pp. 164-170, 1990.
- Nelson, J. C., *Selective Laser Sintering: A Definition of the Process and an Empirical Sintering Model*, Ph.D. dissertation, The University of Texas at Austin, 1993.
- Shi, S. (Xue) and Barlow, J. W., "Measurement of the Thermal Conductivity of Powders by Two Different Methods," In *Solid Freeform Fabrication Symposium Proceedings*, 1993.
- Vail, N. K., Barlow, J. W., and Marcus, H. L., "Silicon Carbide Preforms for Metal Infiltration by Selective Laser Sintering of Polymer Encapsulated Powders," In *Solid Freeform Fabrication Symposium Proceedings*, 1993.
- Xue, S. and Barlow, J. W., "Models for the Prediction of the Thermal Conductivities of Powders," In *Solid Freeform Fabrication Symposium Proceedings*, pp. 62-69, 1991.

## Acknowledgments

We acknowledge financial support of this work from DARPA-ONR grant N0014-92-J-1394.